scientific reports

Check for updates

OPEN

Coupled simulation study of CO_2 adsorption in coal matrix based on CT-derived representative elementary volume (REV)

Chunhua Wang[1,2,3], Qingsong Li[2,3], Fuqiang Ren[1,2,3]✉, Jiannan Wang[1,2], Jie Wang[1,2,3], Xin Song[1,2,3], Yichao Lin[1,2,3], Huaiqian Liu[2,4], Yuxuan Wu[4], Jianping Tu[4] & Bin Li[4]

To enhance the safety and reliability of geological CO_2 sequestration, this study proposes a finite element coupling simulation method based on representative elementary volume (REV) models reconstructed from industrial CT imaging. The objective is to simulate gas migration and stress response within the coal matrix under CO_2 adsorption conditions. The authentic three-dimensional internal structure of coal was acquired via industrial CT scanning, and the optimal REV scale was determined as 60 × 60 × 60 voxels through gradient error analysis. A multi-physics coupling model incorporating seepage, adsorption, and mechanical behavior was established and implemented on the COMSOL platform to perform numerical simulations under varying adsorption durations and injection pressures of 6 MPa. The results indicate that the adsorption-induced swelling of the matrix leads to a redistribution of internal stresses, exhibiting a directional transfer from fractures toward the matrix. The stress response of the coal demonstrates a nonlinear "increase-then-decrease" trend: the fracture domain stress increases from 0.66 to 0.73 MPa in the first day and then decreases to 0.54 MPa at 7 days. These findings offer both technical support and theoretical foundations for elucidating the multi-field coupling mechanisms in coal during CO_2 sequestration and for the development of robust numerical simulation methodologies.

Keywords CO_2 adsorption, Coal fractures, Finite element simulation, Industrial CT, Multi-physics coupling

As global climate change intensifies, geological carbon dioxide (CO_2) sequestration has garnered widespread attention as a critical strategy for achieving carbon neutrality[1]. Among potential sequestration sites, abandoned coal mines are considered ideal due to their abundant spatial capacity and controllable seepage pathways[2,3]. However, under prolonged exposure to high-pressure CO_2, the internal structure of coal inevitably undergoes alterations, manifesting in phenomena such as fracture propagation and stress redistribution. These changes may undermine coal seam stability and elevate the risk of leakage, thereby posing serious safety concerns for long-term storage operations. Consequently, elucidating the effects of CO_2 adsorption on the structural integrity of coal is essential to ensuring the sustained stability of sequestration projects.

Although extensive experimental studies have demonstrated that CO_2 adsorption can lead to coal degradation, traditional experimental techniques still face significant limitations, including low spatial resolution, difficulty in controlling variables, and high data variability. These challenges hinder the accurate characterization of CO_2 distribution and behavior within coal matrices. In contrast, numerical simulation has emerged as a pivotal tool due to its efficiency and controllability, enabling detailed analysis of the interaction between CO_2 and coal. In recent years, researchers have developed a range of adsorption–seepage–mechanical coupling models using finite element (FEM) and computational fluid dynamics (CFD) approaches. By systematically varying parameters such as injection pressure, confining pressure, moisture content, fracture geometry, and pore structure, these models evaluate the impacts of CO_2 injection on coal strength, permeability, and stress distribution. For example, Wang et al.[4] used the COMSOL platform to simulate the mechanical response of coal under varying confining pressures during CO_2 exposure, revealing that increasing the confining pressure from 0 to 30 MPa can effectively

[1]Guizhou Mine Safety Scientific Research Institute Co., Ltd, Guiyang 550025, Guizhou, China. [2]Guizhou Coal Mine Design Research Institute Co., Ltd, Guiyang 550025, Guizhou, China. [3]Guizhou Provincial Laboratory of Intelligent Development and Efficient Utilization of Energy, Guiyang 550000, Guizhou, China. [4]State Key Laboratory of Digital Intelligent Technology for Unmanned Coal Mining, Anhui University of Science and Technology, Huainan 232001, China. ✉email: 190183934@qq.com; 406598671@qq.com

offset the strength reduction induced by CO_2 adsorption. Kumar et al.[5] conducted a parametric analysis on the relationship between injection pressure and mechanical properties using digital rock models. Zhou et al.[6] extending the analysis to include coal moisture content, found that higher moisture levels significantly reduce the compressive strength of coal.

To enhance simulation precision, Liu et al.[7] proposed a variable saturation model. This model was validated by combining Langmuir adsorption theory with field monitoring data, confirming its efficacy in predicting pressure evolution during the injection process. Yu et al.[8] conducted CO_2 injection simulations under different pore arrangement conditions based on actual coal seam structures, revealing characteristics that suggest a higher risk of CO_2 leakage in fractured regions. Niu et al.[9] developed an anisotropic permeability model and indicated that the direction of cleat orientation in coal markedly affects the migration behavior of CO_2. Teng et al.[10] proposed a fully coupled model of structural deformation, seepage, and adsorption, finding that while higher injection pressures may improve sequestration efficiency, they also intensify coal damage and deformation, thereby increasing the risk of gas leakage.

At present, the numerical simulation research of the interaction between coal and rock with CO_2 still has key technical bottlenecks, which is difficult to meet the precision requirements of engineering practice. First, most studies use ideal structural models such as "parallel plate fractures" and "cylindrical pores", ignoring the inherent multi-scale pore characteristics and structural plane effects of coal and rock-Liu et al.[11] confirmed through nitrogen adsorption experiments that real coal and rock pores can be clearly divided into adsorption pores (< 100 nm) and seepage pores (>100 nm). The connectivity and migration resistance of the two types of pores are significantly different. However, the ideal structural model cannot quantify the impact of this difference on CO_2 seepage, resulting in a deviation of 1 to 2 orders of magnitude between the simulation results and the actual seepage rate. Secondly, discontinuous features such as primary fractures and structural planes are common in coal and rocks. Li et al.[12] pointed out in a study on the rockburst mechanism of coal and rocks containing structural planes that stress will transfer directionally near the structural planes, which will then change the crack expansion paths and fluid migration channels. However, traditional models do not consider such structural effects, making it difficult to capture the uneven process of CO_2 accumulating preferentially in high-permeability channels and slowly diffusing into the matrix. Finally, in multi-physical field coupled simulation, traditional methods are often divorced from the real structural parameters of coal and rock. Li et al.[13] found through microseismic and electromagnetic radiation monitoring that there is dynamic feedback between the energy release and pore evolution of coal and rock under stress, and the ideal model cannot reflect the regulation of this feedback on permeability, resulting in the inability to accurately predict the seepage stability during CO_2 storage.

In summary, although current numerical simulation techniques have made significant strides in the study of CO_2-coal interactions, most research still employs idealized fracture structures and does not fully account for the heterogeneity and complex geometry of coal structures. To address this, the present study reconstructs actual three-dimensional digital rock cores based on industrial CT images, creating finite element coupling models on the basis of real fracture structures revealed by CT reconstruction. This work simulates fluid pressure diffusion and coal stress response under CO_2 adsorption conditions. The research outcomes are expected to provide theoretical foundations and technical support for the safety assessment of CO_2 sequestration projects and the optimization of injection strategies.

Numerical modeling method

To delve into the influence of CO_2 adsorption duration and pressure on the structural and mechanical properties of coal, this study reconstructs the actual internal geometry of the coal matrix based on industrial CT imaging. It combines finite element modeling with multi-physics field coupling simulation methods to construct a comprehensive numerical simulation system for CO_2 migration and coal response. Model development utilizes the COMSOL Multiphysics platform and is deployed on a high-performance computing cluster, with the SLURM job scheduler facilitating efficient parallel solving.

Overview and processing methods of industrial CT scanning systems

To construct a geometric model that reflects the true internal structure of coal, this study employs an industrial CT scanning system to obtain three-dimensional images of the coal sample prior to adsorption. The system utilizes a cone-beam scanning approach, the working principle of which is depicted in Fig. 1. The scanning method uses a fixed X-ray source and detector, while the specimen rotates around an axis. Its core advantage is acquiring a 3D projection dataset via a single rotation, which improves X-ray source utilization and shortens scanning time. Additionally, the cone-beam scanning mechanism endows it with isotropic voxel resolution—that is, axial and horizontal resolution are consistent—effectively improving the clarity and spatial detail representation of the reconstructed images.

The physical basis of CT imaging stems from the attenuation effect that occurs when X-rays interact with the object under examination. As X-rays penetrate an object, their intensity diminishes due to the absorption and scattering of photons. This process follows Lambert-Beer's law[14], which states that the attenuation of intensity along the path of the rays is directly proportional to the material's linear attenuation coefficient. This attenuation model forms the physical foundation for collecting CT projection data and subsequent three-dimensional reconstruction.

Post-scanning, the slice images can undergo calibration and analysis using post-processing software, with the specific workflow as follows:

(1) Utilizing filtering algorithms to denoise the images, thus enhancing the clarity of fracture boundaries;

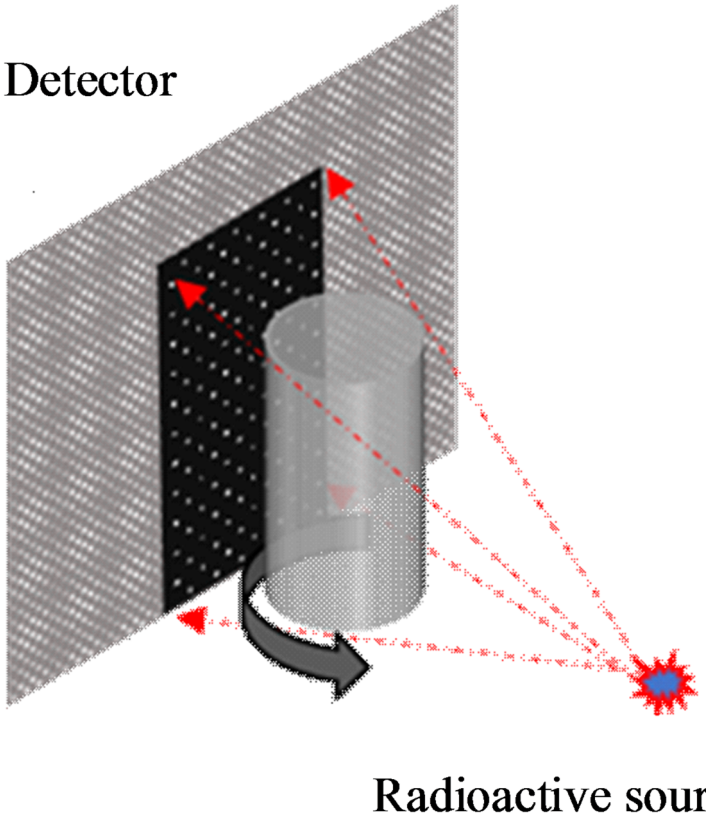

Fig. 1. Principle of cone-beam CT scanning.

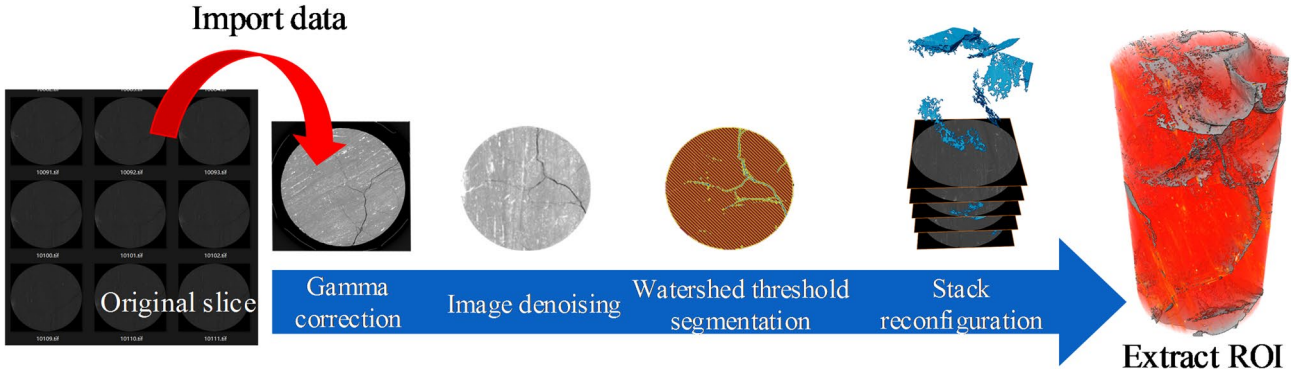

Fig. 2. CT post-processing workflow.

(2) Employing grayscale thresholding to segment the fracture regions and extract geometric characteristic parameters of fractures;
(3) Generating three-dimensional geometric models from two-dimensional slice images through reconstruction techniques to visually analyze fracture characteristics under adsorption conditions, as depicted in Fig. 2.

Overview of numerical simulation software and system

This research utilizes the COMSOL Multiphysics platform to perform numerical simulations analyzing the CO_2 adsorption process in coal.

The platform, based on the finite element method (FEM), discretizes continuous physical systems into several elements. By introducing shape functions, unknown field variables are transformed into a solvable set of algebraic equations, thus enabling the simulation of complex boundary conditions and nonlinear multi-physics processes[15,16]. The principle of finite elements is illustrated in Fig. 3.

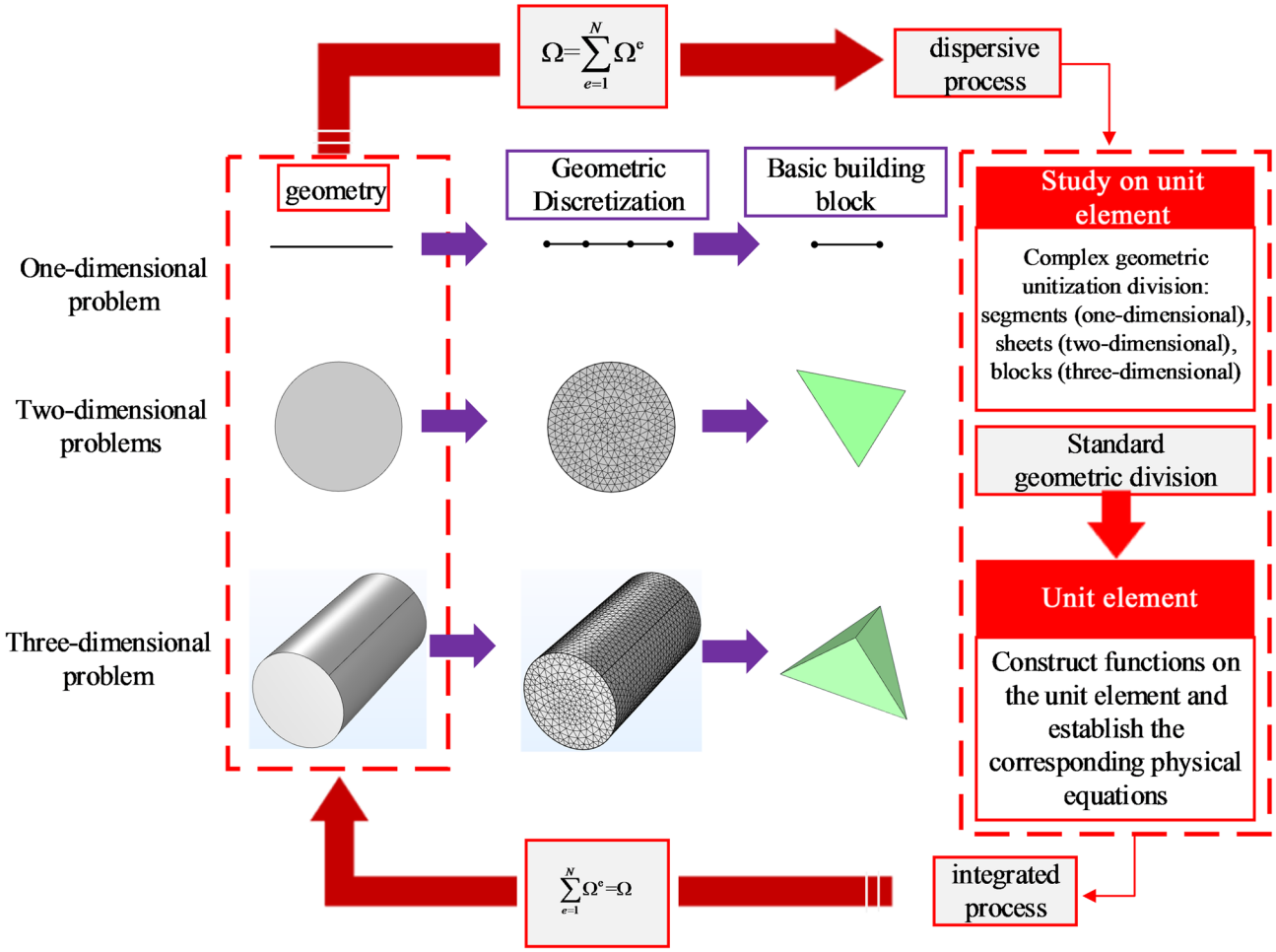

Fig. 3. Schematic of finite element principles.

Additionally, COMSOL software offers excellent meshing capabilities for three-dimensional models and compatibility with three-dimensional models reconstructed from industrial CT scanning. With straightforward model-building import features, high-precision simulations of coal fracture structures can be achieved.

To satisfy the demands of large-scale three-dimensional simulations, the model is deployed on a high-performance computing cluster (HPCC) platform and utilizes the SLURM job scheduling system for dynamic resource allocation and parallel solving. SLURM's modular structure supports task scheduling and node load balancing, enhancing simulation efficiency. Figure 4 displays the system architecture and actual running logs, significantly reducing solution times and improving simulation precision.

Extraction and construction of representative elementary volume (REV) models

In multi-physics simulations of CO_2 adsorption and coal response, accurate construction of the geometric model is key to simulation precision. Coal fracture structures exhibit high heterogeneity and irregular spatial distribution. Directly using entire CT scan data to establish simulation models could lead to poor mesh quality, heavy computational burden, and severe boundary distortion. To balance the representativeness of the structure with numerical efficiency, this study introduces the concept of Representative Elementary Volume (REV). Stable structural areas within the coal CT images are cropped and extracted to be used in subsequent multi-field coupling simulations.

The necessity of constructing REV

Coal internal fracture morphology is complex, exhibiting typical characteristics such as "multi-scale nesting, strong discontinuity, and large spatial variability." Traditional simulations often simplify coal as a regular fracture model, which fails to reflect its true evolutionary process. Therefore, establishing a real geometric model based on CT scans is key to enhancing the credibility of simulations. However, within the entire three-dimensional scanning body, there exist discontinuous structures such as CT artifacts and isolated noise points (as shown in Fig. 5); regions with excessive sparsity or density of fracture structures; and large voxel models that are computationally intensive and difficult to converge[17].

Thus, it is necessary to ensure statistical representativeness while extracting and selecting stable structural areas to construct an REV model that conforms to the true physical characteristics. The selected REV should not

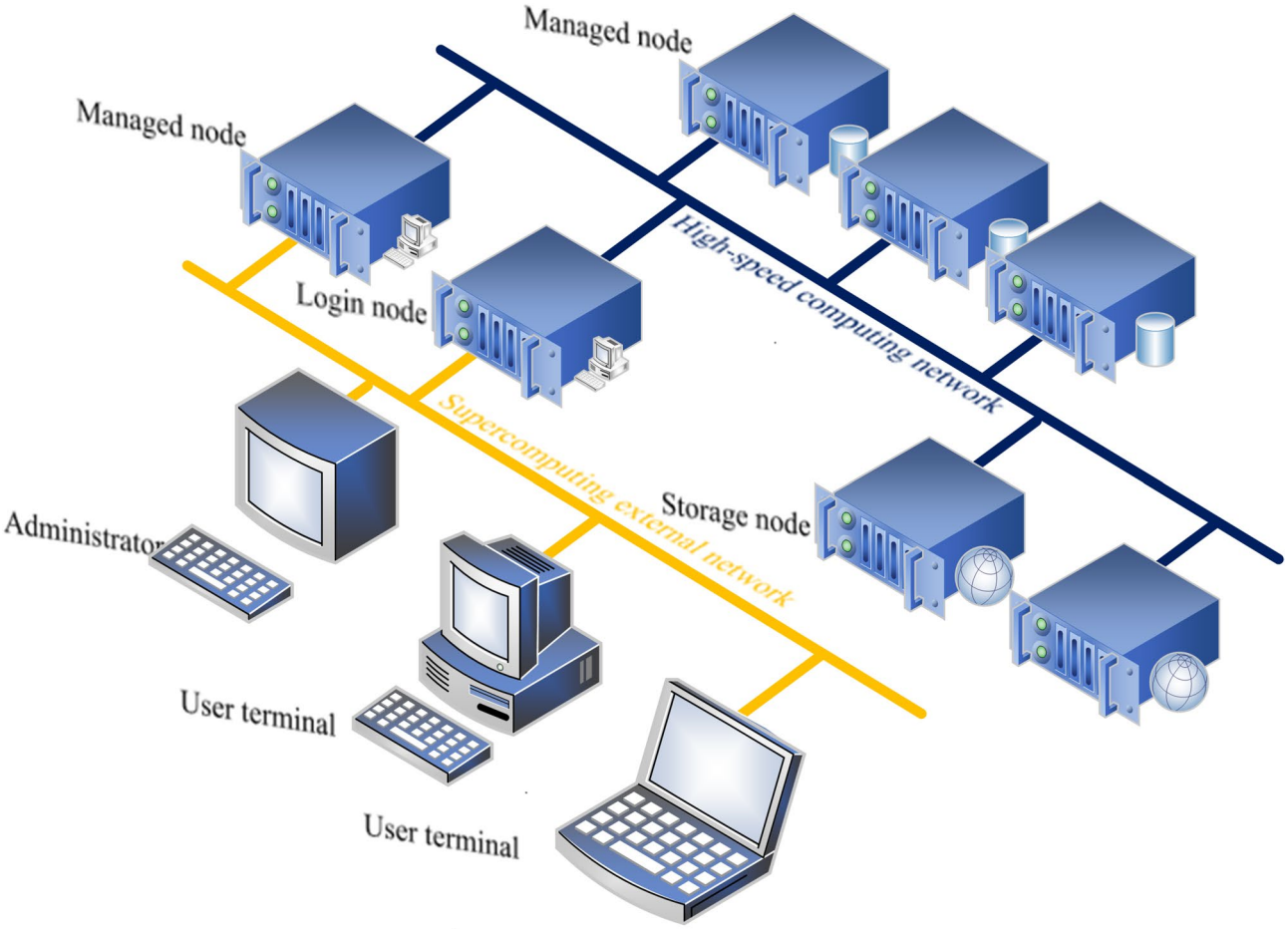

Fig. 4. High-performance cluster computing (HPCC) system architecture.

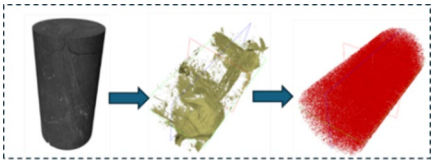

Fig. 5. Extraction of digital rock core noise.

only possess typical fracture morphologies but also reflect the average response characteristics of the coal body on a certain scale.

REV extraction process

REV extraction is based on the following three principles: the geometric structure within the selected volume should have statistical uniformity; the variation range of parameters such as fracture porosity, connectivity, and fractal dimension within the extracted area should tend toward stability; and the size should be as small as possible to reduce computational costs while ensuring representativeness.

To ensure that the geometric modeling area is statistically representative, the relationship between fracture porosity and image cropping size is explored. By plotting the curve of fracture porosity changes at different cubic sizes (as shown in Fig. 6), it can be seen that as the size of the cube increases, the fracture porosity initially fluctuates and then stabilizes. When the cropping size reaches approximately 60 voxels, the fracture porosity becomes stable, and the fluctuation amplitude significantly decreases, indicating that this size can serve as an effective representative elementary volume (REV). A reasonable REV can not only accurately characterize the statistical properties of coal fractures but also avoid the randomness of results due to too small a model size, or computational redundancy due to too large a model size.

To further optimize the selection process of REV, this article introduces the gradient error analysis method, which quantitatively assesses the change gradient of key physical quantities (such as fracture porosity,

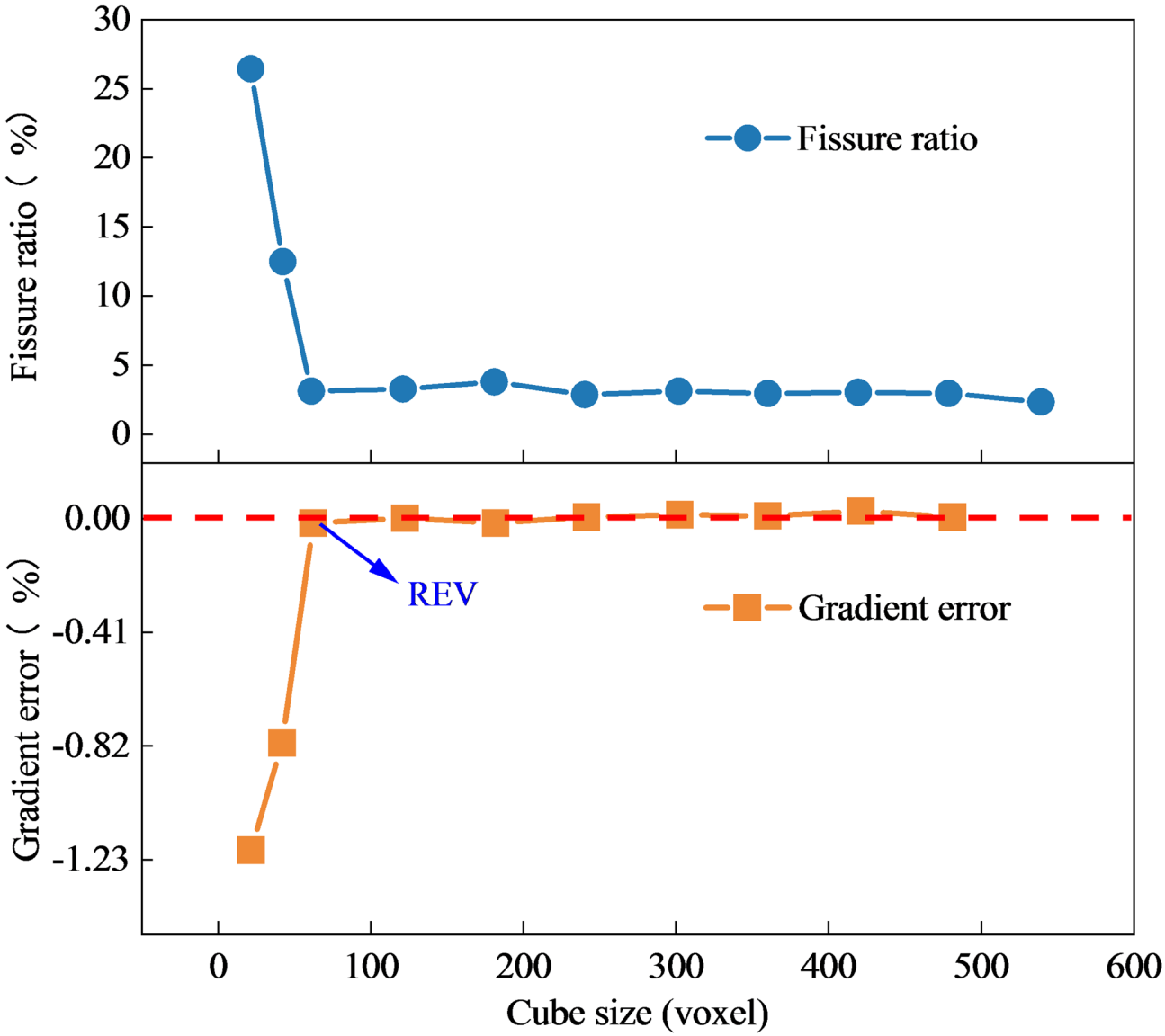

Fig. 6. Analysis results for REV selection.

permeability, stress distribution) under different REV sizes. The method identifies the scale where the error is minimized and the change tends toward stability by calculating the rate of change of physical quantities with varying REV sizes, thus determining the optimal REV size. The core idea of gradient error analysis is to find the "physical quantity change stability zone," which corresponds to the minimum volume size when the gradient error value approaches zero. At this point, the model achieves a good balance between structural representativeness, simulation accuracy, and computational efficiency. Compared to the traditional trial-and-error method, gradient error analysis has advantages such as strong objectivity, good adaptability, and clear error control. It can be widely used in different coal body structures and multi-physics field simulations to optimize the REV scale. The gradient error can be defined as[18]:

$$e_r = \frac{k_{i+1} - k_{i-1}}{\delta(k_{i+1} + k_{i-1})} \tag{1}$$

where er represents the gradient error; k_{i+1} and k_{i-1} are the outputs corresponding to the i + 1 and i − 1 samples, respectively; δ is voxel increment at adjacent REV scales. In this study, the REV scale increases in steps of 20 voxels when less than 60 × 60 × 60 voxels, δ = 20, and then 60 voxels are taken as steps, δ = 60.

The calculation process is as follows. When the REV scale is 60 × 60 × 60 voxels, the fracture porosity at subsequent scales is close to that at this time (as shown in Fig. 6). At this time, $k_{i+1} - k_{i-1} \approx 0$, e_r tends to 0, the gradient error begins to stabilize, therefore, the REV size for the simulation model is set to 60 × 60 × 60 voxels.

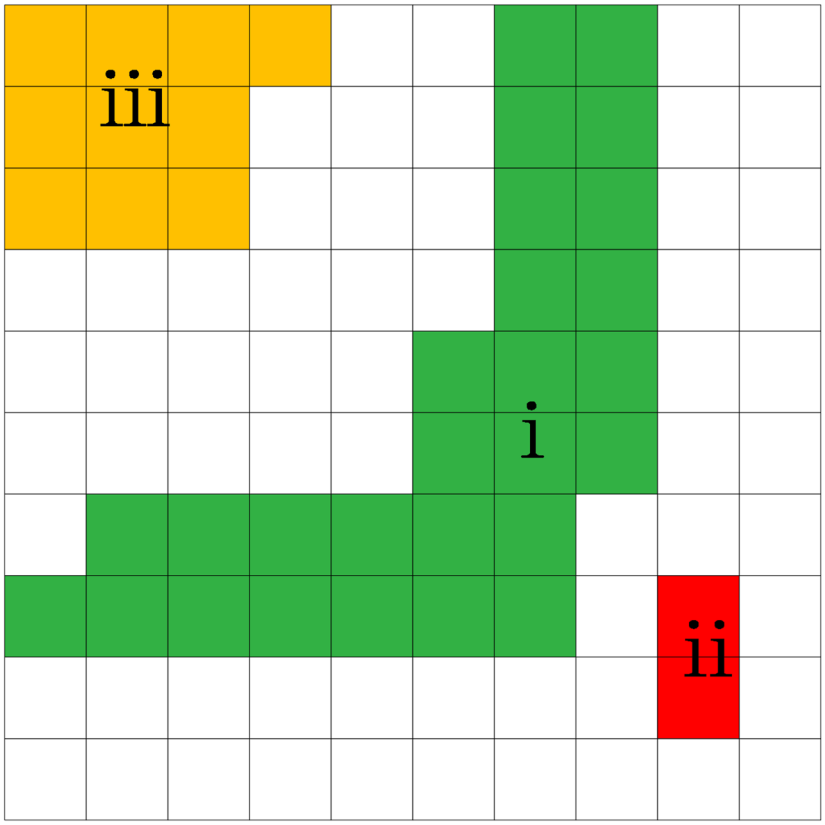

Fig. 7. Schematic diagram of fracture connectivity.

Construction of the geometric model

In the reconstruction process of coal structure, the internal fracture structures can be divided into three types[19] (as shown in Fig. 7): i—connected fractures, ii—internally isolated fractures, and iii—single boundary contact isolated fractures.

Among these, connected fractures traverse the interior of the coal matrix, forming a fracture network that dominates fluid migration and mechanical responses; these are of significant research interest. In contrast, isolated fractures (types ii and iii) often segment the coal matrix domain into multiple disconnected regions, leading to increased computational redundancy and time cost in simulations, as well as the potential for cumulative numerical errors that reduce the overall model accuracy.

To improve simulation efficiency and consistency, it is necessary to extract REV containing cracks and matrix from the sample (Fig. 8a), and isolated cracks need to be addressed appropriately (Fig. 8b). For internally isolated fractures, a common approach is to fill them in order to ignore their effects and maintain the continuity of the coal matrix domain; for single boundary contact fractures, a decision is made based on their contact area and geometric shape on whether to convert them into boundary conditions or to eliminate them directly. This strategy not only retains the structural authenticity of the coal fracture network but also effectively simplifies the geometric model, enhancing the stability and computational efficiency of numerical simulations.

This experiment focuses on the simulation of CO_2 gas migration under matrix and fracture conditions. Therefore, minerals within the coal are considered part of the matrix, with the entire coal divided into two parts: fractures and matrix. To restore the gas-solid coupling occurrence state of the coal, an air domain is set outside the REV, with the size of the air domain set to $70\times70\times70$ voxels. The essence of fluid-solid coupling is the interaction between fluid dynamics and solid mechanics. Its important feature is the two-way influence between two-phase media: deformed solids will move or deform under the action of fluid loads, and this deformation will in turn change the distribution of the flow field. Without a clearly modeled air domain, the software will not be able to calculate key field variables. Then using mesh processing software, a model like the one shown in Fig. 9 can be generated. In the COMSOL software, the preliminarily meshed file is data interfaced, and the grid quality is visually inspected for zero-value color blocks (Fig. 9). If low-quality meshes are found, secondary repair and optimization are performed until there are no red meshes in the model entity, which means the model mesh division is suitable for simulation calculations.

Control equations and parameter settings

Construction of control equations

To systematically describe the migration and diffusion behavior of CO_2 adsorption in coal and its induced structural stress response, this paper constructs a coupled multi-physical field mathematical model based on the

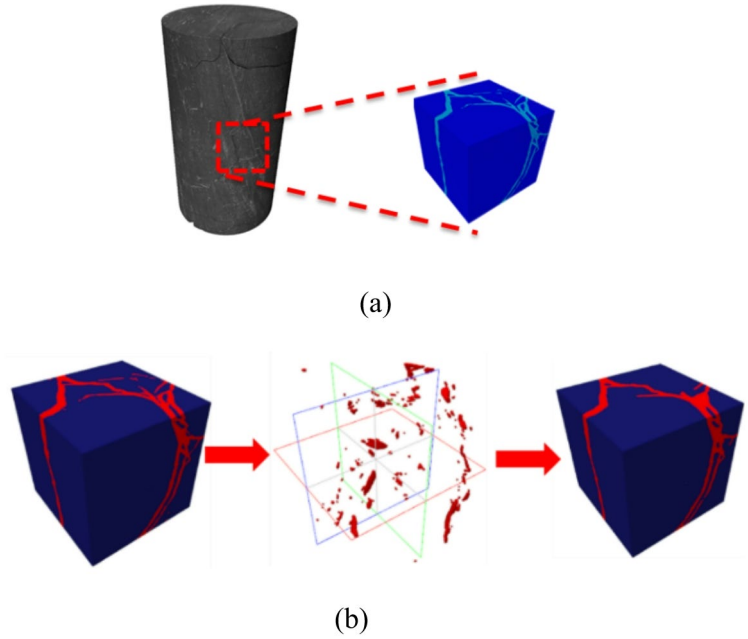

Fig. 8. Model preprocessing. (**a**) Schematic of REV cutting, (**b**) treatment of isolated fractures.

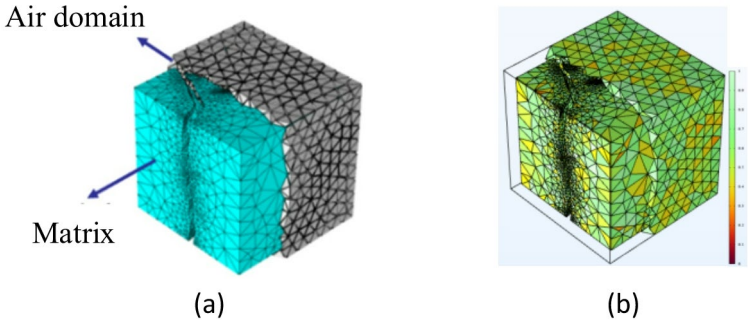

Fig. 9. Digital rock core mesh processing. (**a**) Simulation geometric model, (**b**) mesh quality.

theories of porous media mechanics and seepage mechanics. The model primarily includes the solid momentum conservation equation, fluid mass conservation equation, Darcy's law, and a density expression based on fracture porosity to replicate the dynamic evolution of the stress field and seepage field in coal under CO_2 adsorption.

To characterize the mechanical response of coal under the action of CO_2 pressure and external body forces, the following momentum conservation expression based on Newton's second law is introduced[20]:

$$\rho \frac{\partial^2 \mathrm{u}_0}{\partial t^2} = \nabla \cdot \mathrm{S} + \mathrm{F}_v \tag{2}$$

where ρ is the effective density of the coal body, in kg/m^2; u_0 represents the solid skeleton displacement field, in meters; S is the total stress tensor, in Pascals; F_v is the external body force, in Newtons.

Assuming slow and steady diffusion of CO_2 gas, the fluid mass conservation equation is expressed as[21]:

$$\frac{\partial}{\partial t}(\varepsilon_{\mathrm{p}} \rho_f) + \nabla \cdot (\rho_f \mathrm{u}_1) = Q_m \tag{3}$$

where ε_p is the fracture ratio, in percent, which is considered zero due to the attributes of the REV as fracture characteristics have been extracted, hence no additional fracture parameter influences the coal matrix; ρ_f is the fluid density, in kg/m^2; u_1 is the fluid velocity vector, in m/s; Q_m represents the external mass source or sink term (such as CO_2 injection volume). This equation simplifies to:

$$\nabla \cdot (\rho_f \mathrm{u}_1) = Q_m \tag{4}$$

According to Darcy's law, under low flow conditions, velocity is directly proportional to the pressure gradient, and is expressed as[22]:

$$u_1 = -\frac{k}{\mu}\nabla p \tag{5}$$

where k is the coal permeability, in m^2; μ is the fluid viscosity, in Pa s; p is the fluid pressure field. Substituting Eqs. (4–5) into Eqs. (4–4), we obtain the final CO_2 migration control equation:

$$-\nabla \cdot \left(\rho_f \frac{k}{\mu}\nabla p\right) = Q_m \tag{6}$$

This expression, driven by the pressure gradient, accurately describes the spatiotemporal distribution of CO_2 in the coal fracture structure.

In a coupled fluid-solid system, the dynamics response of the system is determined by both the solid and fluid masses. The following density expression is introduced to represent the overall density distribution of the fracture-matrix mixed system[23]:

$$\rho = \varepsilon_p \rho_f (1 - \varepsilon_p)\rho_s \tag{7}$$

where ρ_s is the density of the coal matrix, in kg/m^3. This relationship implies that with fluid permeation and by setting $\varepsilon_p = 0$, the overall system density simplifies to $\rho = \rho_s$. Substituting this density relation into the momentum conservation Eqs. (2–4), we obtain the revised coupled fluid-solid momentum equation:

$$(\varepsilon_p \rho_f + (1 - \varepsilon_p)\rho_s)\frac{\partial^2 u_0}{\partial t^2} = \nabla \cdot S_s + F_v \tag{8}$$

Finally, by combining Eqs. (4–6) and (4–8), we establish the core set of control equations that describe the seepage and structural response of coal under the combined effects of CO_2 adsorption pressure and time, providing a theoretical foundation for subsequent coupled numerical simulations.

Applicable boundary for simplified matrix fracture porosity

In this study, the core basis for simplifying the matrix fracture rate to 0 is the functional zoning characteristics of coal and rock pores: through industrial CT scanning and gray threshold segmentation, the coal body is clearly divided into "fracture domain" and "matrix domain", among which the fracture domain contains all macro fractures and some micro fractures that can participate in seepage flow (porosity 8.1–8.3%), while the matrix domain is a dense skeleton, containing only primary pores with a pore size of less than 10 nm. Such micropores are limited by the compactness of the coal and rock skeleton, and can only store CO_2 through physical adsorption and cannot form a continuous seepage channel. Their contribution to the migration of CO_2 is negligible, so it is reasonable to set the fracture rate to 0.

The simplified applicable coal types are bituminous coal and anthracite with low porosity (< 10%): the connectivity of matrix pores and fracture networks is weak, and the diffusion rate of CO_2 in the matrix is much lower than that in the fractures. The seepage rate, the influence of the matrix on the overall seepage field is negligible. For lignite and long-flame coal with high porosity (> 20%), transition pores (50–100 nm) are developed in the matrix and are connected to the fractures, and CO_2 can migrate through the transition pores of the matrix. At this time, a dual porous medium model needs to be adopted. The matrix is regarded as a "porous medium" and endowed with a non-zero fracture rate. The simplification of this study is not applicable to such coals.

Parameter setting and simulation boundary condition determination

To accurately obtain the initial mechanical properties of coal in the unadsorbed state, this paper conducts uniaxial compression tests on three sets of parallel coal samples, measuring and statistically analyzing key physico-mechanical indicators such as compressive strength, elastic modulus, and density. By examining the characteristics of the stress-strain curves, the deformation and failure behaviors of coal during the loading process are evaluated, providing reliable data for material parameter settings in subsequent numerical simulations. Related experimental data are shown in Fig. 10; Table 1.

Notes:

1. The average density of 1437.5 kg/m^3 in the table directly corresponds to the coal matrix density ρs in governing Eqs. (7) and (8). This density is the skeleton density of the dry coal sample, which is consistent with the model assumption that ' the matrix domain is a dense solid ', ensuring the accuracy of the density parameter in the fluid-solid coupling calculation;
2. The average elastic modulus of 1.18 GPa corresponds to Young's modulus that characterizes the elastic deformation of the coal matrix in the conservation equation of solid momentum (2). It is used to construct the elastic matrix in Eq. (8) and calculate the stress-strain relationship of the solid skeleton;
3. The average peak strength of 12.3 MPa is used to constrain the simulation boundary conditions: the maximum stress of the coal body in the simulation is set to not exceed 12.3 MPa to ensure that the model is in the elastic deformation stage (to avoid coal body damage interfering with the seepage and stress coupling

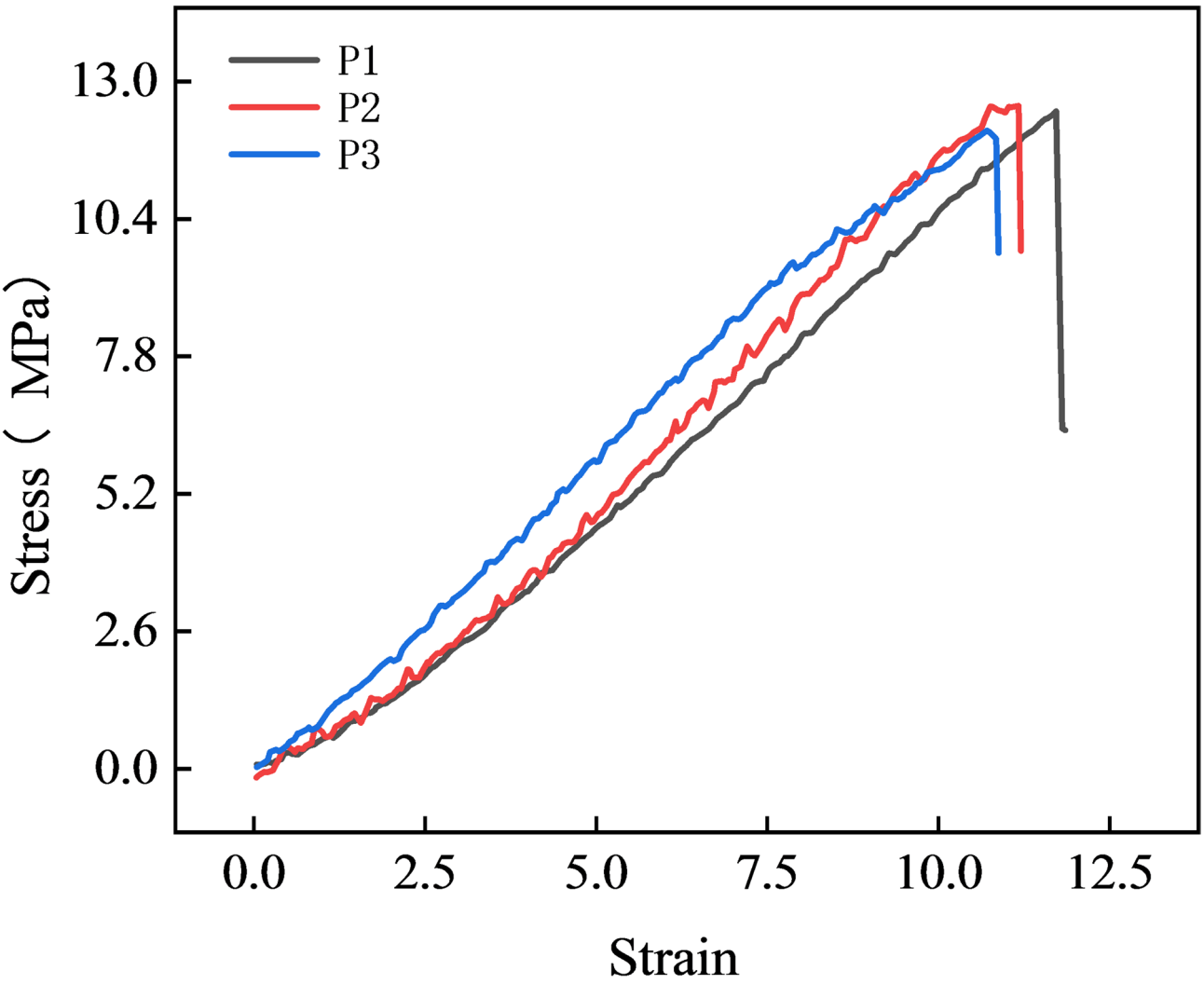

Fig. 10. Stress–strain curve.

Sample No.	P1	P2	P3	Mean
Diameter × Height mm×mm	25.01 × 49.10	25.12 × 50.11	24.99 × 49.56	25.04 × 49.56
Mass g	35.3	35.1	34.9	35.1
Density kg/m^3	1463.4	1413.3	1435.7	1437.5
Elastic Modulus GPa	1.21	1.24	1.19	1.18
Peak strength MPa	12.4	12.5	12.0	12.3

Table 1. Sample physical parameter Measurement.

process), which is consistent with the results of Section "Evolution of coal stress distribution under CO_2 adsorption" "The maximum stress in the fracture zone is 0.73 MPa (much lower than 12.3 MPa);

4. The average diameter × height 25.04 × 49.56 mm in the table is used to verify the representativeness of the CT scan samples and ensure that the structural characteristics extracted by REV are consistent with the statistical characteristics of the macro coal samples.

One side of the air domain is set as the gas inlet, while the surfaces of the air domain are constrained with roller supports, and all faces in the matrix are set as free displacement faces, with detailed settings shown in Fig. 11.

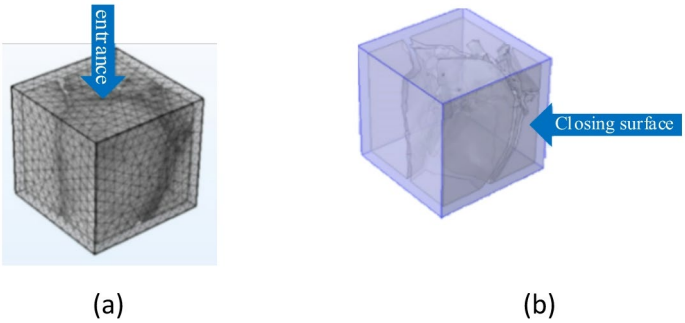

Fig. 11. Boundary setting schematic diagram. (**a**) Injection face setting, (**b**) constraint face setting.

Parameter Name	Value
Coal Density ρ_s/kg m^{-3}	1437.51
CO_2 density ρ_f/kg m^{-3}	1.784
Coal permeability k/m^2	1×10^{-18}
CO_2 fluid viscosity μ/Pa s	1.38×10^{-5}
CO_2 injection pressure p_0/MPa	6

Table 2. Parameter settings.

In the fluid module of COMSOL software, the basic parameters are set using a transient solver for computation, with time steps set to (0, 2, 7). Key parameters are shown in Table 2.

Simulation results and analysis

CO_2 migration and distribution characteristics

Using the post-processing capabilities of COMSOL, the evolution curve of CO_2 gas pressure inside the coal under a 6 MPa adsorption condition was obtained, as shown in Fig. 12.

Simulation results indicate significant heterogeneity in gas migration. CO_2 preferentially infiltrates and accumulates rapidly along permeability-favored pathways—fracture domains and the external surfaces of the matrix domain, as seen in Fig. 13. Driven by seepage and diffusion, gas migrates from these favored regions to the matrix interior, achieving full equilibrium after 7 days.

Compared to the fracture domain, where pressure quickly responds and redistributes, the rise and diffusion of CO_2 pressure within the matrix domain show a distinct lag. This phenomenon profoundly reveals the inherent impediment effect of the coal matrix on CO_2 migration, which is fundamentally due to the matrix's high density and low diffusion characteristics. This impediment effect induces a significant non-equilibrium stress state in the initial stages of adsorption; the fracture domain exhibits local high-pressure saturation due to rapid gas filling, while the deep matrix maintains a low-pressure area close to its initial state.

Evolution of coal displacement field distribution under CO_2 adsorption

Based on a deformation analysis of the representative elementary volume (REV) bisecting plane (see Fig. 14), the study found that prolonged CO_2 adsorption time leads to increased displacement and deformation in the coal fracture domain. However, the deformation induced by CO_2 adsorption within the REV matrix domain shows significant disparity. The specific transfer mechanism of deformation is as follows: when the internal expansion deformation of the matrix domain becomes apparent, its deformation effect transfers to the adjacent fracture faces. During this process, influenced by external boundary constraints and matrix expansion, some fracture edges shift away from the matrix domain. Conversely, if the expansion deformation in the matrix domain is not pronounced, the region is mainly controlled by boundary compression, with the fracture faces being predominantly influenced by the gas-phase CO_2 pressure.

As the CO_2 pressure accumulation and expansion deformation in the matrix domain continue, the deformation effect is further transmitted to the fracture domain. Regions of the matrix with higher expansion push the adjacent fracture faces outward and prompt the transfer of pressure within the fracture domain to the fracture faces of the matrix domain with lower expansion. This uneven deformation causes an overall shift in the fracture domain and exerts additional compression on the fractures in the constrained matrix areas, leading to increased fracture aperture and volume (Fig. 15).

In summary, CO_2 adsorption not only directly induces expansion in the matrix domain but also regulates the evolution of the fracture domain through a stress transfer-feedback mechanism. This process enhances the expansion and connectivity of the fracture network during adsorption.

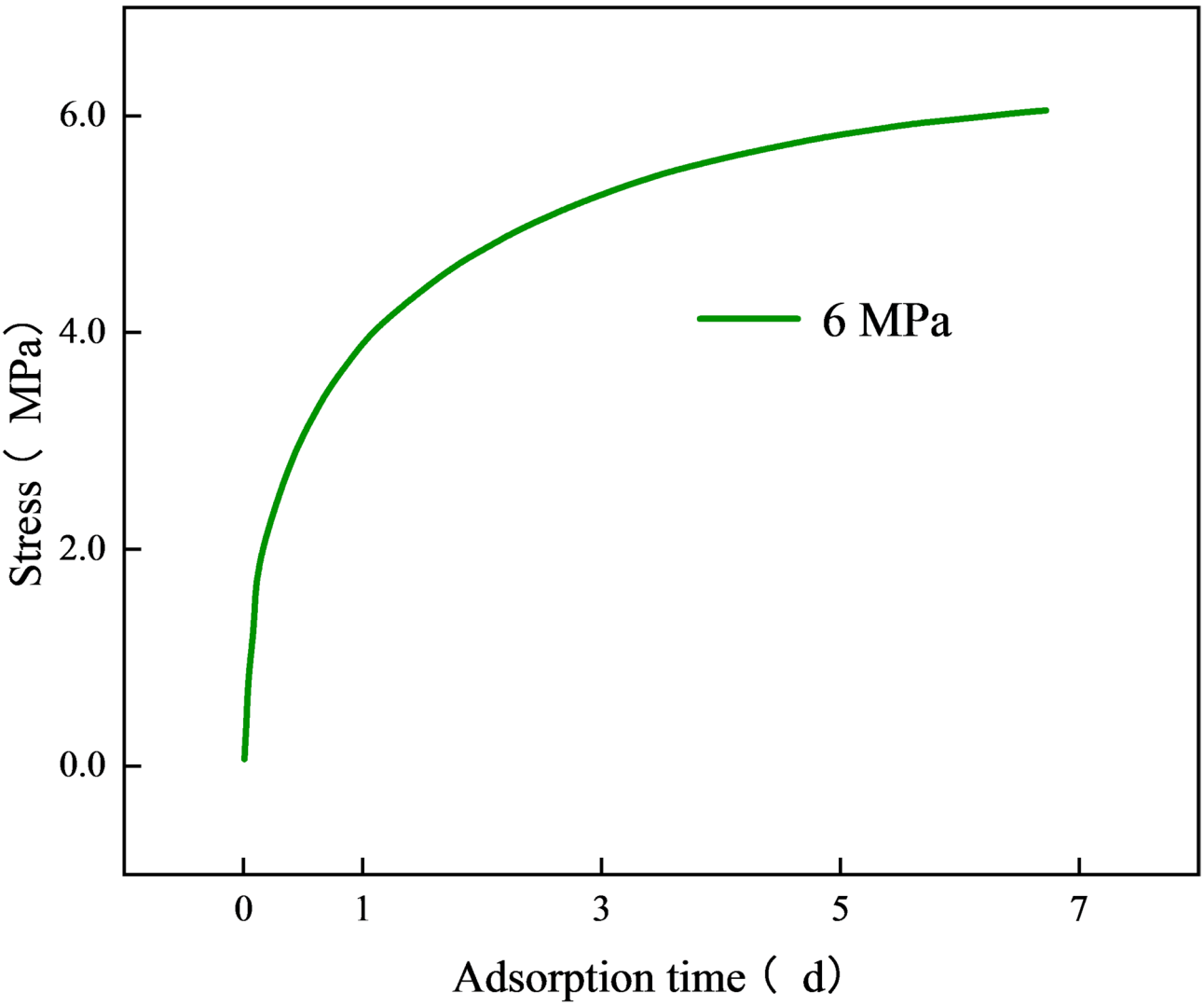

Fig. 12. Change in CO_2 pressure during REV adsorption.

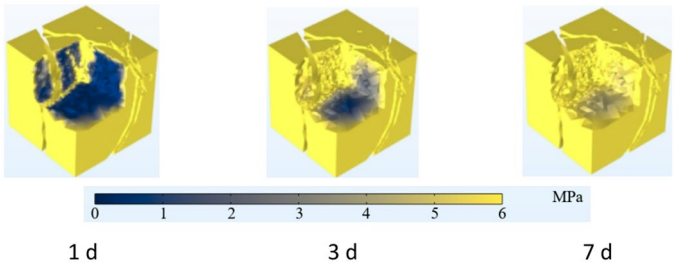

Fig. 13. Contour maps of CO_2 pressure change during REV adsorption.

Evolution of coal stress distribution under CO_2 adsorption

The analysis of the homogenized stress field evolution in the coal body throughout the full CO_2 adsorption cycle (0–7 days) under a 6 MPa injection condition (Fig. 16) reveals that in the initial stage of adsorption (0–1 day), the average stress within the fracture domain rapidly increased from 0.66 to 0.73 MPa. This reflects the significant expansion response and structural damage effects induced by the instantaneous accumulation of high-pressure CO_2 in the high-permeability fracture network. As the adsorption time extended from 1 to 7 days, fracture stress displayed a non-monotonic evolution: the average stress gradually decreased from its peak of 0.73–0.54 MPa (at 7 days). This stage fundamentally represents a stress redistribution process dominated by gas diffusion from

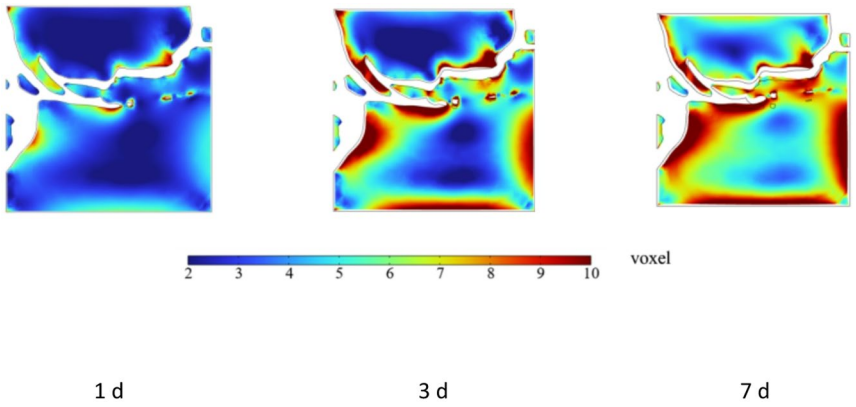

Fig. 14. Displacement contour map of REV sections.

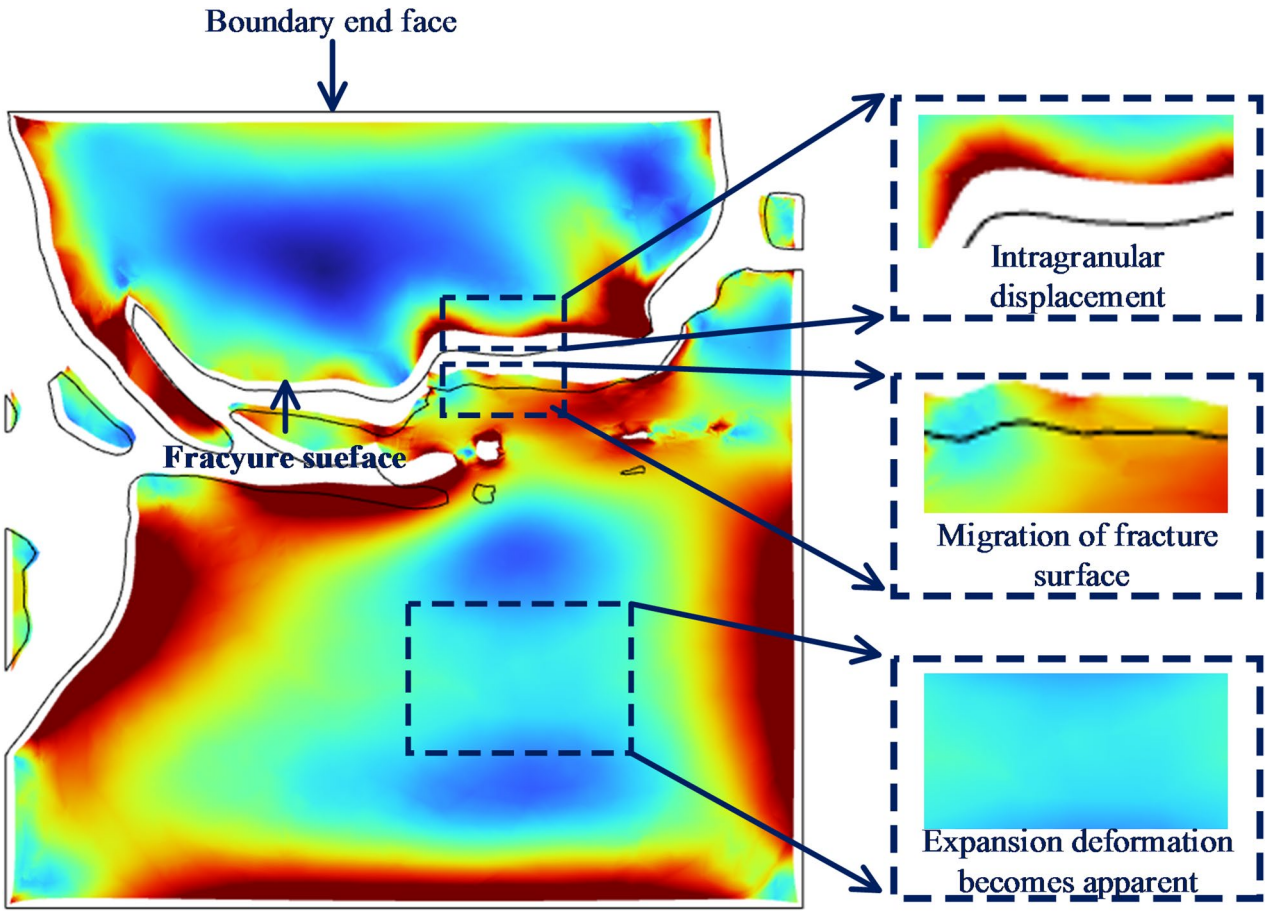

Fig. 15. Schematic diagram of REV displacement principle.

fractures into the matrix domain: on one hand, the expansion stress generated by the matrix's continuous CO_2 adsorption is transferred to the fracture-matrix interface, forming a directional constraint that inhibits fracture propagation; on the other hand, the homogenization of the CO_2 pressure field significantly alleviates localized high-pressure concentrations within the fractures. The coupled mechanism of diffusion-expansion ultimately leads to a dynamic evolution of stress in the fracture domain, characterized by an initial increase followed by a decrease.

Moreover, high-pressure conditions (6 MPa) intensify fracture propagation through two pathways: firstly, they amplify the extent of irreversible fracture expansion caused by instantaneous gas saturation during the initial adsorption stage; secondly, they notably weaken the constraining effect of matrix expansion stress on fractures during the middle and late stages, making it difficult to counteract the dominant expansion established

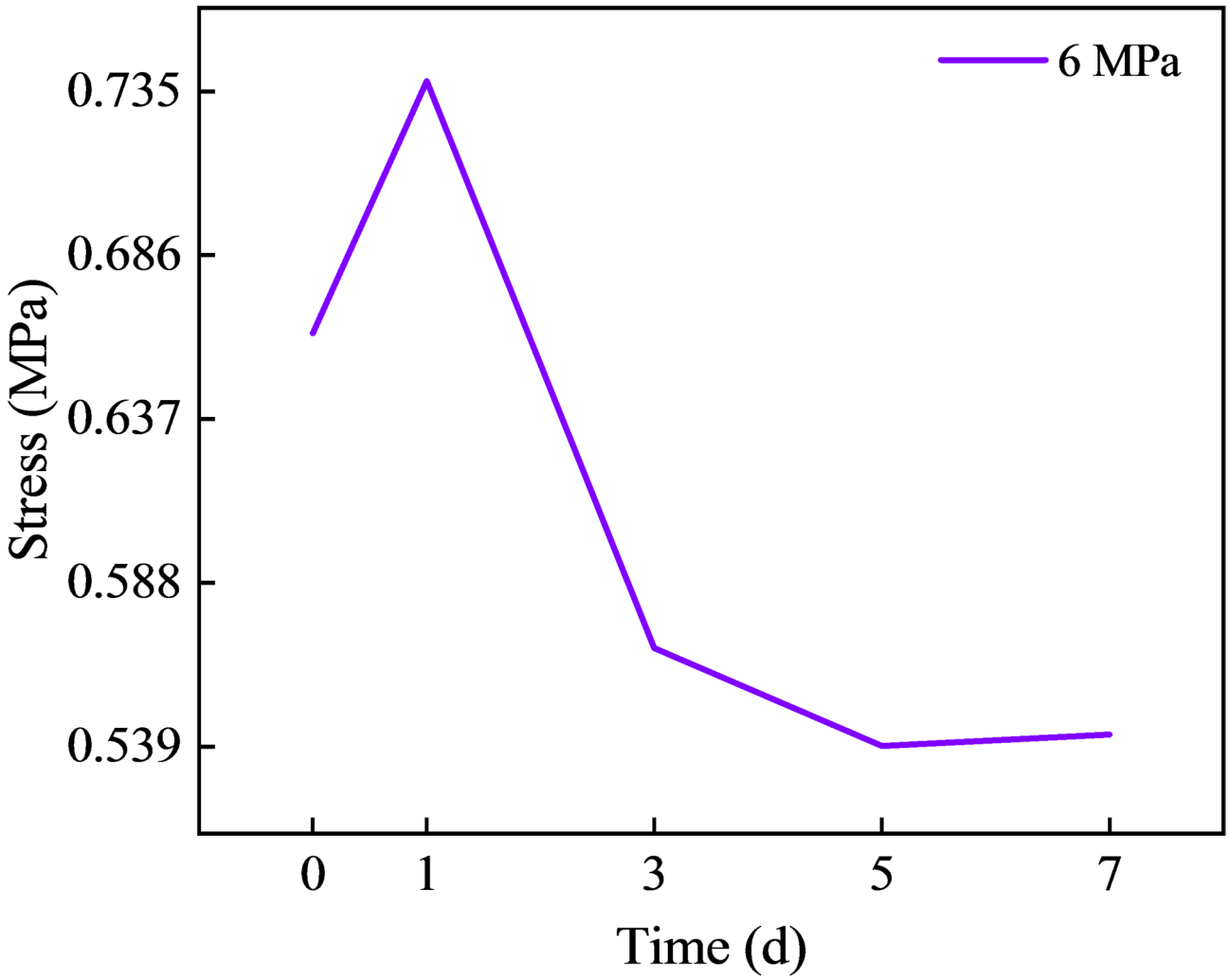

Fig. 16. Change in REV stress distribution under CO_2 influence.

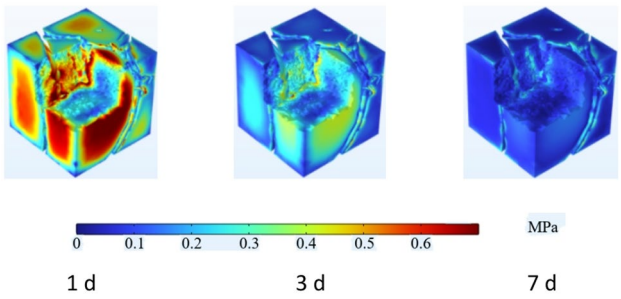

Fig. 17. Contour maps of REV stress distribution change under CO_2 influence.

by high-pressure gas in the initial stage, as shown in the 7-day stress contour map in Fig. 17. This weakening of the constraint is the fundamental mechanical cause behind the more intense fracture propagation and the continued enhancement of connectivity under high-pressure CO_2 injection.

Conclusions

(1) This study integrates industrial CT scanning and the finite element method to develop a multi-physics numerical simulation model that couples CO_2 adsorption, seepage, and mechanical behavior in coal. By incorporating a representative elementary volume (REV) extraction approach with the optimal scale identified as

$60 \times 60 \times 60$ voxels, the model reconciles the structural heterogeneity of coal with computational efficiency, achieving a balance between fidelity in structural representation and feasibility in numerical simulation.

(2) During the initial adsorption stage (1 day), CO_2 rapidly accumulates in fracture zones, while diffusion into the matrix domain is significantly delayed. This pressure disparity induces non-uniform stress redistribution, which promotes fracture propagation and enhances fracture connectivity. Over 7 days of adsorption, the stress within the fracture domain exhibits a nonlinear "increase-then-decrease" trend: rising from 0.66 to 0.73 MPa in the early stage, then decreasing to 0.54 MPa. This forms a complex dynamic feedback loop between CO_2 migration and coal structural deformation.

(3) The modeling methodology and simulation framework established herein provide a robust technical pathway and theoretical foundation for analyzing fracture evolution, stress redistribution, and sequestration risk prediction in coal formations. By quantifying the spatiotemporal dynamics of CO_2 migration and stress response, this work offers actionable insights for optimizing geological CO_2 storage strategies and evaluating long-term safety.

Data availability

The datasets used and/or analyzed during the current study are available from the corresponding author on reasonable request.

Received: 4 September 2025; Accepted: 7 November 2025
Published online: 27 November 2025

References

1. Yuan, L. et al. Construction of green, low-carbon and multi-energy complementary system for abandoned mines under global carbon neutrality. *J. China Coal Soc.* **47**(06), 2131–2139 (2022).
2. Li, L. L. et al. CO_2 sequestration in Ucg cavities: Research progress and future development trends. *Chin. J. Theor. Appl. Mech.* **55**(03), 732–743 (2023).
3. Liu, L. et al. CO_2 storage-cavern construction and storage method based on functional backfill. *J. China Coal Soc.* **47**(03), 1072–1086 (2022).
4. Wang, W. W. et al. Mechanical properties of coal-rock combined bodies under the action of ScCO2: A study of damage and failure mechanism. *Eng. Fail. Anal.* **156**, 107807 (2024).
5. Kumar, D. H., Mishra, M. K. & Mishra, S. 3D modelling of coal deformation under fluid pressure using COMSOL Multiphysics. *J. Eng. Sci. Technol. Rev.* **10**(6), 3923859 (2017).
6. Zhou, X. P., Jiang, D. C. & Zhao, Z. Engineering digital evaluation of micro-pore water effects on mechanical and damage characteristics of sandstone subjected to uniaxial, cyclic loading–unloading compression by 3D reconstruction technique. *Rock Mech. Rock Eng.* **55**(1), 147–167 (2021).
7. Liu, G. X. & Andrei, V. S. Modeling of carbon sequestration in coal-beds: A variable saturated simulation. *Energy Convers. Manage.* **49**(10), 2849–2858 (2008).
8. Yu, R. et al. Study on the mechanism of liquid carbon dioxide fracturing and permeability enhancement technology in low permeability thick coal seam. *Geofluids* **2022**(1), 1–20 (2022).
9. Niu, Q. H. et al. Experimental and numerical model of anisotropic permeability and CO_2 injectivity of coal during CO_2 enhanced coalbed methane recovery process. *Front. Earth Sci.* **10**, 1042477 (2023).
10. Teng, T. et al. Feasibility of carbon dioxide geological storage in abandoned coal mine: A fully coupled model with validated multi-physical interactions. *Int. J. Greenh. Gas Control* **138**, 104256 (2024).
11. Liu, S. M. et al. Experimental study of effect of liquid nitrogen cold soaking on coal pore structure and fractal characteristics. *Energy* **275**(7), 127470 (2023).
12. Li, X. L., Chen, S. J., Li, Z. H. & Wang, E. Y. Rockburst mechanism in coal rock with structural surface and the microseismic (MS) and electromagnetic radiation (EMR) response. *Eng. Fail. Anal.* **124**(6), 105396 (2021).
13. Li, X. L. et al. Rock burst monitoring by integrated microseismic and electromagnetic radiation methods. *Rock Mech. Rock Eng.* **49**(11), 4393–4406 (2016).
14. Shen, L. & Xing, Y. Implementation techniques and acceleration of DBPF reconstruction algorithm based on GPGPU for helical cone beam CT. *Nuclear Tech.* **33**(11), 857–862 (2010).
15. Wang, G. et al. Numerical simulation on non-Darcy seepage of CBM by means of 3D reconstruction based on computed tomography. *J. China Coal Soc.* **41**(04), 931–940 (2016).
16. Wang, L. et al. Mechanical properties and crack propagation law of coal under different CO_2 adsorption time. *J. Min. Sci. Technol.* **9**(06), 964–976 (2024).
17. Min, K. B., Jing, L. R. & Stephansson, O. Determining the equivalent permeability tensor for fractured rock masses using a stochastic REV approach: Method and application to the field data from sellafield, UK. *Hydrogeol. J.* **12**(5), 497–510 (Hydrogeol. J.).
18. Li, J. H. et al. Permeability tensor and representative elementary volume of saturated cracked soil. *Can. Geotech. J.* **46**(8), 928–942 (2009).
19. Miao, J. *3D Reconstruction and Seepage Simulation of Macropores Structure in Low Permeability Coal* (Henan Polytechnic University, 2017).
20. Fang, H. H., Sang, S. X. & Liu, S. Q. Establishment of dynamic permeability model of coal reservoir and its numerical simulation during the CO_2-ECBM process. *J. Petrol. Sci. Eng.* **179**, 885–898 (2019).
21. Fang, H. H., Sang, S. X. & Liu, S. Q. The coupling mechanism of the thermal-hydraulic-mechanical fields in CH4-bearing coal and its application in the CO_2-enhanced coalbed methane recovery. *J. Petrol. Sci. Eng.* **181**, 106177 (2019).
22. Wang, Y. K. *Experimental Study on CO_2 Replacement of Methane and Numerical Simulation Analysis* (China University of Mining and Technology, 2016).
23. COMSOL AB. *COMSOL Multiphysics® Porous Media Flow Module User's Guide, Version 6.3 [EB/OL]* (COMSOL AB, Stockholm, 2024).

Acknowledgements

This work was supported by the Guizhou Provincial Science and Technology Program (Grant No. QKHZC [2023]001); the Guizhou Provincial Program for Innovation-Oriented Talent Team Development (Grant No. QKHFWQY [2022]010); the Guizhou Provincial Science and Technology Support Program (General Project, Grant No. QKHZC [2025]027); and the Guizhou Provincial Science and Technology Support Program (Enter-

prise Collaboration, Grant No. QKHFWQY [2022]010).

Author contributions

Chunhua Wang: Funding acquisition, conceptualization. Qingsong Li: Writing—original draft. Fuqiang Ren: Methodology, formal analysis. Jiannan Wang: Resources. Jie Wang: Visualization, data curation. Xin Song: Methodology. Yichao Lin: Investigation. Huaiqian Liu: Writing—review and editing. Yuxuan Wu: Visualization. Jianping Tu: Writing—review and editing. Bin Li: Software.

Funding

Authors did not receive any funding for this work.

Declarations

Competing interests

The authors declare no competing interests.

Additional information

Correspondence and requests for materials should be addressed to F.R.